The Performance of an Attic Radiant Barrier for a Simulated Minnesota Winter

H. Chen **T. Larson, Ph.D.** **R.W. Erickson, Ph.D.**

ABSTRACT

The effectiveness of attic radiant barrier systems in reducing heat loss through the ceiling was evaluated by theoretical and experimental approaches under designated winter conditions. Both approaches gave very low reductions in heating load due to a radiant barrier system. For the theoretical calculations, assuming no ventilation, the placement of a radiant barrier caused the natural convective heat transfer to increase by an amount almost equal to the radiative heat flux reduction. The heat flux reduction decreased with an increase in the R-value of ceiling insulation and outside temperature. For the experimental results, where ventilation did exist, there was no statistically significant reduction in heat flux with the radiant barrier either on top of the ceiling insulation or attached to the underside of the attic roof.

Frost developed on the underside of the horizontal perforated radiant barrier when the exterior temperature was 10°F (−12°C) or less.

INTRODUCTION

Heat transfer in attic spaces occurs mainly through radiation and convection. The quantity of radiation depends on the temperatures of surfaces facing each other in the attic (the top surface of the ceiling insulation and the bottom surface of the roof sheathing) and their emissivities, while convection depends on the surface temperatures, the attic air temperature and velocity, and the heat transfer directions.

In predominantly cooling climates, the roof temperature is normally very high due to the absorption of solar radiation. Also, the emissivities of the surfaces within the attic are normally high, close to 0.9. These factors lead to radiant heat transfer, but a relatively small amount of heat transfer in the attic space occurs by convection due to downward heat flow. Therefore, radiant barrier (RB) systems have been used to reduce ceiling heat gain; commonly used radiant barriers are aluminum foils with emissivities around 0.03. It has been shown that an RB reduces summer ceiling heat gains by about 16% to 42% (DOE 1991) with R-19 insulation, or up to a 10% reduction in the cooling costs.

Levins and Karnitz (1988) studied the effectiveness of RB systems in reducing heat loss during the heating season in a mild climate. The effectiveness was less than that for heat gain in the warm season, and the systems performed more effectively with R-11 and R-19 levels of attic insulation than with R-30. Horizontally installed barriers were more effective than truss-mounted barriers in reducing heating loads.

Little research has been done on the effectiveness of RB systems in reducing heat loss through the ceiling in a cold climate typical of Minnesota. The effect of an RB on convective heat transfer in the heating situation has not been discussed much in the literature. Forest (1990) studied attic RB performance in a cold climate—Alberta, Canada. He found about a 5% reduction in the total annual heat loss through the roof/ceiling, which amounted to a 1% savings in the total heating load. When interior air was allowed to leak into the cold attic space, moisture condensed and frost formed on the underside of the RB and in the fiberglass insulation that supported the RB.

For the research herein, the effectiveness of RBs in reducing heat loss under cold-climate conditions was evaluated both theoretically and experimentally. The effect of placing the RB on top of the insulation, upon the relative humidity below the RB, was also evaluated.

THEORETICAL APPROACH

During the winter in cold climates, there are three modes of heat transfer from the house to the exterior through the attic system: conduction, convection, and radiation. Conduction dominates through the ceiling and roof, while convection and radiation dominate in the attic space. Figure 1 gives a simplified presentation of attic heat flow. For the following analysis, heat transfer through the ceiling/roof assembly is assumed to be one-dimensional. Based on an analysis by McQuiston and Parker (1988), heat flux through the attic can be expressed as

$$Q_{ceil} = Q_{rad} + Q_{conv} = Q_{roof} + Q_{vent} \qquad (1)$$

or

$$\frac{(T_{in} - T_{s-ai})}{R_{ceil}} = \frac{\sigma\left(T_{s-ai}^4 - T_{s-br}^4\right)}{\frac{1}{\varepsilon_1} + \frac{1}{\varepsilon_2} - 1} + h_c(T_{s-ai} - T_a) = \frac{T_{s-br} - T_{out}}{R_{roof}} + Q_{vent} \qquad (2)$$

Hung Chen is a student, **Timothy Larson** is a research scientist, and **Robert W. Erickson** is a professor at the University of Minnesota.

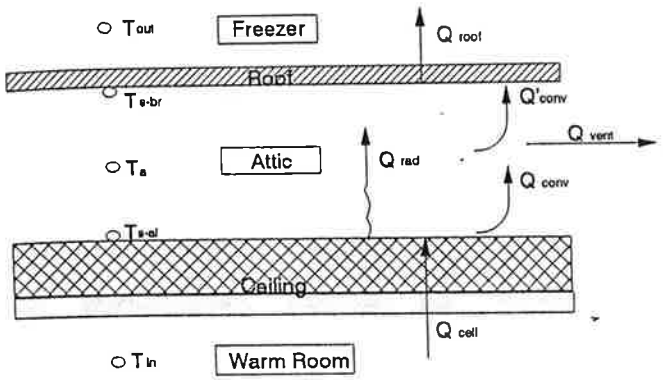

Figure 1 Simplified schematic of attic heat flow.

where

Q_{ceil} = heat transfer through ceiling, Btu/h·ft^2 W/m^2),
Q_{rad} = radiation between ceiling and roof surfaces, Btu/h·ft^2 (W/m^2),
Q_{conv} = convective heat transfer in attic space, Btu/h·ft^2 (W/m^2),
Q_{roof} = heat transfer through roof, Btu/h·ft^2 (W/m^2),
Q_{vent} = heat loss by attic ventilation, Btu/h·ft^2 (W/m^2-),
T_{in} = temperature of the heated room air, °R (K),
T_{out} = temperature of the outside air, °R (K),
$T_{s\text{-}ai}$ = temperature of the top surface of the ceiling insulation, °R (K),
$T_{s\text{-}br}$ = temperature of the bottom surface of the roof sheathing, °R (K),
T_a = temperature of the attic air, °R (K),
R_{ceil} = thermal resistance between T_{in} and $T_{s\text{-}ai}$, h·ft^2·°F/Btu (m^2·°C/W),
R_{roof} = thermal resistance between $T_{s\text{-}br}$ and T_{out}, h·ft^2·°F/Btu (m^2·°C/W),
h_c = convection coefficient in attic space, Btu/h·ft^2·°F (W/m^2·°C),
ϵ_1 = emissivity on the top surface of the ceiling insulation,
ϵ_2 = emissivity on the bottom surface of the roof sheathing,
σ = Stefan Boltzmann constant, 0.1713 × 10^{-8} Btu/h·ft^2·°R^4 (5.673×10^{-8} W/m^2·K^4).

Equation 2 shows that the quantities of radiative and convective heat transfer depend not only on the emissivities of the facing surfaces but also on their temperatures, which, in turn, are a function of inside and outside air temperature, ceiling and roof insulation, and attic ventilation. Emissivities determine the amount of heat transfer from the top surface of the ceiling insulation to the bottom surface of the roof sheathing. This changes the temperatures of the facing surfaces, which again influence the quantity of convective heat transfer. The effect of an RB can be expressed as

$$\downarrow\epsilon \rightarrow Q_{rad}\downarrow \;\&\; T_{s\text{-}ai}\uparrow \;\&\; T_{s\text{-}br}\downarrow \;\&\; Q_{conv}\uparrow .$$

Thus, the reduction of heat flux due to the RB is actually the combined result of the reduction in radiation and the increase in convection. To show this quantitatively, the radiative and convective heat transfer as affected by an RB system were calculated by Equation 2, with the assumption of no attic ventilation in order to simplify the calculation. The calculations used a T_{out} of 32°F, 0°F, and -20°F (0°C, -17.8°C, and -28.9°C) and ceiling insulation (R_{insu}) values of 19, 38, and 57 h·ft^2·°F/Btu (3.32, 6.64, and 9.96 m^2·°C/W). The values of h_c were calculated using the equation by Lloyd and Moran (1974). The emissivities of the RB, the insulation surface, and the roof undersurface are 0.03, 0.9, and 0.8, respectively. The location of the RB, either on top of the ceiling insulation or on the lower surface of the attic roof, has the same effect on radiative heat transfer. The results obtained are given in Figure 2 and Table 1.

Figure 2 shows that radiation is nearly eliminated with the RB, but the increase in natural convection is about equal to this reduction. As a result, the net effect of the RB on total ceiling heat transfer is very small. Table 1 shows a maximum heat flux reduction of 0.259 Btu/h·ft^2 (0.817 W/m^2) when T_{out} is -20°F (-28.9°C) and R_{insu} is 19 h·ft^2·°F/Btu (3.32 m^2·°C/W). The heat flux reduction decreases with an increase in R_{insu} and T_{out}.

Ventilation varies so much in actual houses that no single value of ventilation is representative, but its effect on heat transfer is easy to depict. An increase in ventilation reduces T_a and increases h_c. Consequently, convective heat transfer is increased and the effectiveness of an RB system is reduced. When ventilation is zero, an RB system is most effective.

In a warm climate, the situation is different. Ventilation reduces the convective heat transfer from the attic air to the ceiling insulation surface, and the h_c is larger for heat flow upward than for heat flow downward. Both of these factors make an RB more effective in reducing cooling loads than in reducing heating loads.

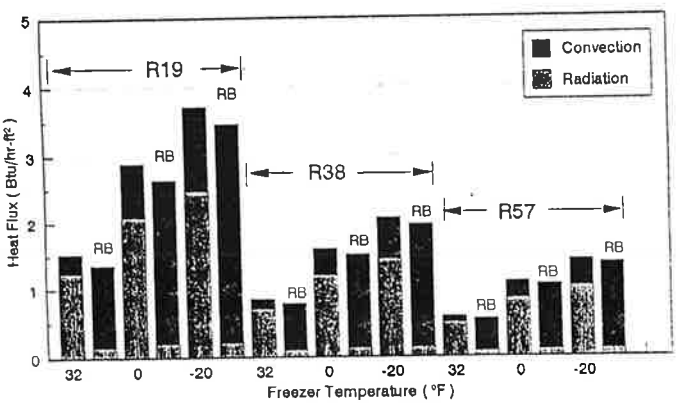

Figure 2 Theoretical heat flux with and without the RB, assuming no attic ventilation.

TABLE 1
Theoretically Calculated Attic Temperature and Heat Flux Data Under the Assumption of No Attic Ventilation

R_{insu}	T_{out}	$T_{s\text{-}ai}$(°F)		Q_{total}(Btu/hr·ft²)		Q_{rad}(Btu/hr·ft²)		Q_{conv}(Btu/hr·ft²)		ΔQ	ΔQ/Q
	(°F)	No RB	RB	No RB	RB	No RB	RB	No RB	RB	(Q_0 - Q)	(%)
	32	36.63	40.21	1.530	1.356	1.240	0.149	0.291	1.207	0.174	11.4
19	0	8.96	13.92	2.880	2.638	2.082	0.200	0.799	2.438	0.242	8.4
	-20	-8.25	-2.93	3.719	3.460	2.476	0.211	1.243	3.249	0.259*	7.0
	32	34.60	37.17	0.846	0.781	0.706	0.096	0.140	0.685	0.065	7.7
38	0	5.09	8.65	1.593	1.502	1.197	0.126	0.396	1.376	0.091	5.7
	-20	-13.26	-9.39	2.058	1.959	1.440	0.133	0.618	1.826	0.099	4.8
	32	33.82	35.86	0.585	0.549	0.497	0.072	0.088	0.477	0.036	6.0
57	0	3.57	6.42	1.101	1.053	0.848	0.095	0.253	0.958	0.048	4.4
	-20	-15.25	-12.11	1.423	1.369	1.026	0.100	0.397	1.269	0.054	3.8

* 1 Btu/hr·ft² = 3.1537 W/m²

EXPERIMENTAL APPROACH

Paraphernalia

The model house (Figure 3) is a heated room with an attic space and is located in a walk-in freezer where it is possible to simulate winter temperatures. The house is 13 ft long by 6 ft wide (39.7 m by 2 m) with a 4/12 sloped shed roof. The attic has two experimental cells, each with a ceiling area of about 6 by 6 ft (2 by 2 m) and contains an air volume of approximately 100 ft³ (2.8 m³). The ceiling of the 2 ft (0.61 m) high warm room is 5/8-in. (15.9-mm) drywall that is attached to the bottom chords of trusses spaced 2 ft (0.61 m) on center. The 6-mil polyethylene vapor retarder was placed between the drywall and the bottom chords of the trusses. Removable fiberglass batts were placed between the bottom chords in direct contact with the vapor retarder. The attic roof is made of 5/8-in. (15.9 mm) plywood. The four fans of the refrigeration system plus another fan were used to minimize the temperature variation throughout the freezer air.

The RB is single faced, with the aluminum foil reinforced by paper. The perforation density is 64 holes/in.², each with a diameter of about 5.9×10^{-3} in. (0.15 mm). The average emissivity of the RB is 0.03. Two heat flux transducers (HFT) and 16 type-T thermocouples were used to measure the heat flux and the temperatures (Figure 4). The HFTs are 1 × 1 ft (310 × 310 mm) with a thickness of 0.0275 in. (0.7 mm). Both surfaces are covered by polyester sheets. An HFT was located centrally in each cell between the bottom chords of two trusses. The influence of the bottom chords of the trusses on heat flux was ignored for simplicity. The HFTs were placed between the drywall and the vapor retarder, and heat sink gel was used between the HFT and the drywall to improve the thermal contact. The thermocouples were placed in the warm room, beneath and above the ceiling drywall, above the ceiling insulation, in the attic space, beneath and above the roof sheathing, and in the freezer. They were located in the same vertical plane between two trusses in the center of each cell. Surface temperature sensors were mounted with paper tape.

A 3^3 factorial design was used to evaluate the heat flux through the ceiling, with each setting replicated. To minimize any error caused by different conditions between the two cells, a random experimental design was used to assign T_{out}, R_{insu}, and the RB locations. Null tests were performed at all of the test settings. The nominal T_{out} values were 32°F, 0°F, and -20°F (0°C, -17.8°C, and 28.9°C); the R_{insu} values were 19, 38, and 57 h·ft²·°F/Btu (3.32, 6.64, and 9.96 m²·°C/W), with average insulation thicknesses of 5.5, 11, and 16.5 in. (140, 280, and 420 mm), respectively. Multiple layers of fiberglass batts were used to achieve R-38 and R-57. The RB was located either on top of the ceiling insulation or just below the roof sheathing. The warm room temperature was maintained at 68°F (20°C) throughout the experiments. To ensure that the thicknesses of the fiberglass batts were the same in both cells and between all chords, a row of marked sticks used for sight leveling of the insulation was installed on the bottom chord of each truss. The density of the fiberglass batt was about 0.604 lb/ft³ (0.038 kg/m³).

To evaluate humidity conditions under the RB, a separate experiment was carried out in which 15 wood samples, each 3/4 in. by 2 in. (19 mm by 50.8 mm) in cross section and 1/4 in. (6.4 mm) along the grain, were used to estimate relative humidity via its correspondence to wood moisture content. They were placed beneath and above the ceiling insulation, in the attic space, and in the

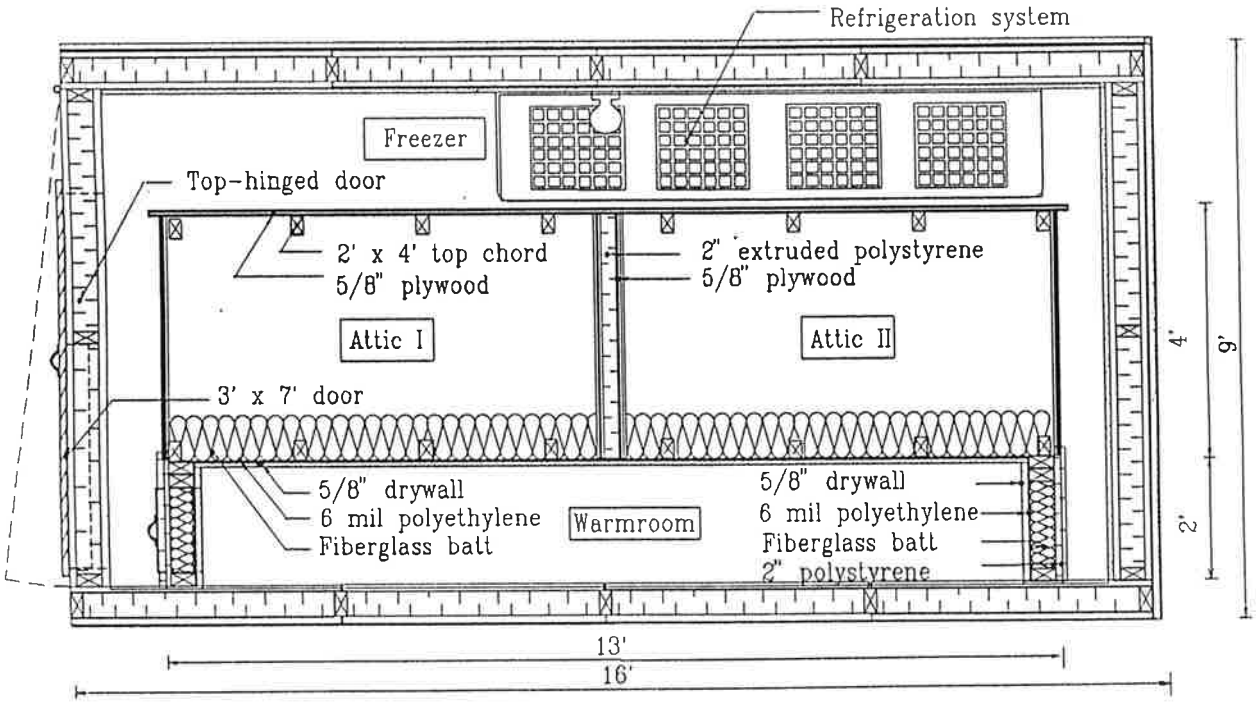

Figure 3 *Construction details of the freezer and the model house.*

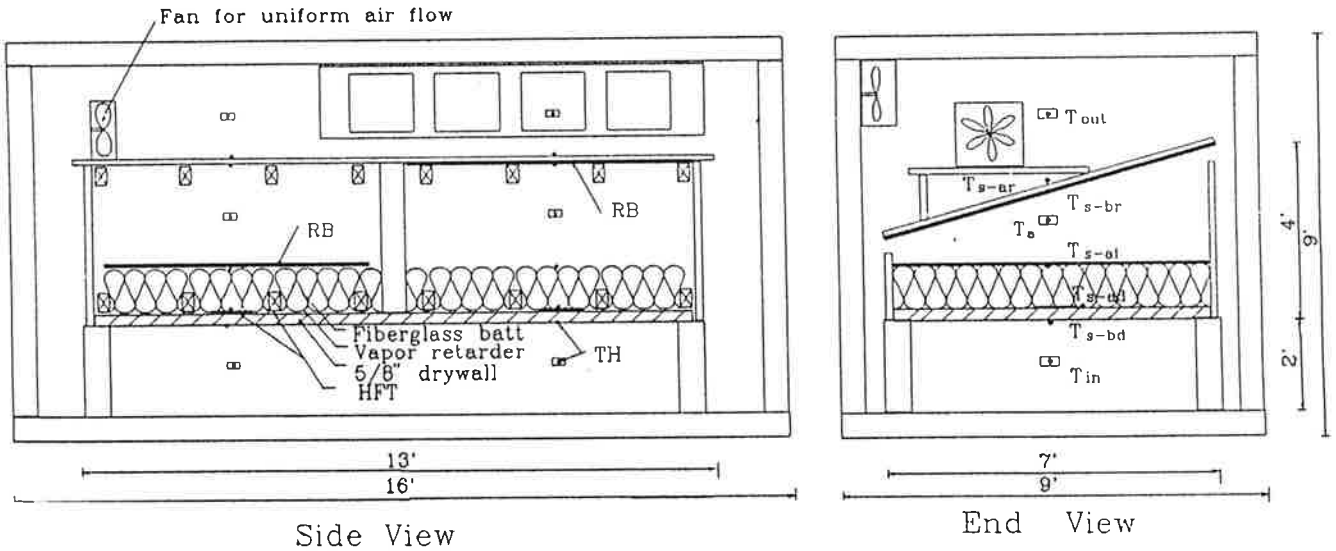

Figure 4 *Model house showing the locations of radiant barriers (RB), heat flux transducers (HFT), and thermocouples (TH).*

warm room (Figure 5). The test conditions selected were T_{out} of 10°F (-12°C) and R_{insu} of 38 h·ft^{2}·°F/Btu (6.64 m^{2}·°C/W) with the RB placed on top of the ceiling insulation.

Data Collection and Calculations

Air temperature in the freezer underwent regular fluctuations between given limits, so the heat transfer through the ceiling also fluctuated. The longest on-off cycle for the refrigeration system was about 30 minutes. Because of these fluctuations, the heat flux and temperature readings were taken every 30 seconds and averaged for five-minute intervals over a three-hour test duration. The freezer ran at set conditions for at least one day prior to any data collection to allow for stabilization.

The data collected by the acquisition system were voltages for the HFTs and direct temperatures for the thermocouples. The heat flux through the ceiling was calculated from the HFT voltage by the following equation (EKO 1990):

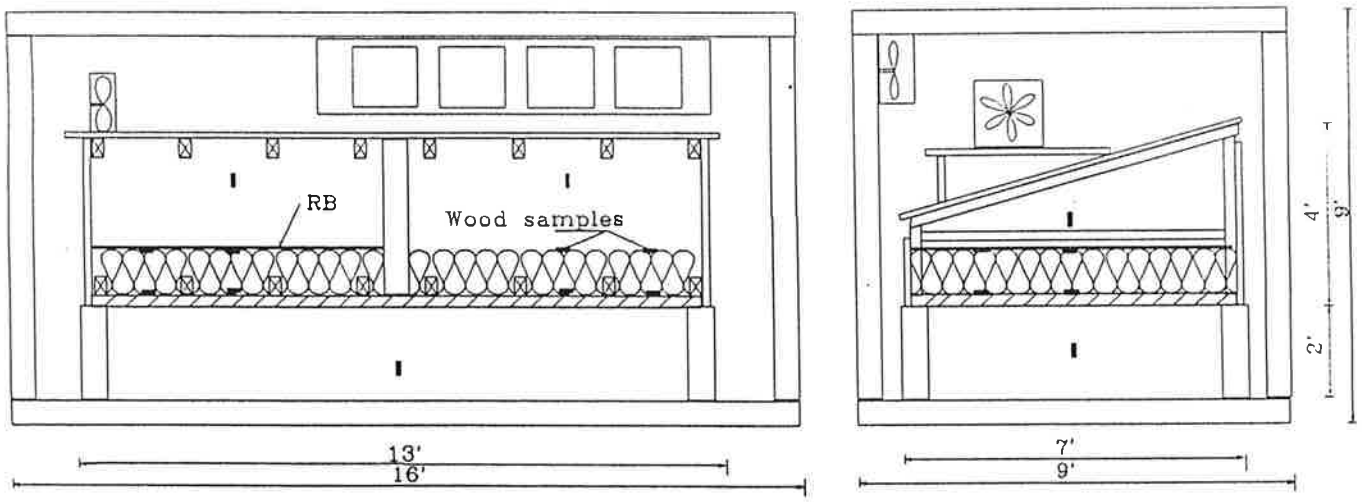

Figure 5 *Model house showing the locations of wood samples.*

$$Q_{ceil} = \frac{E}{C \times \left(1 + (T_{trans} - 68°F) \times 0.0014\,°F^{-1}\right)} \quad (3)$$

where

Q = ceiling heat flux, Btu/h·ft^2 (W/m^2),
E = output voltage, mV,
C = sensitivity of HFT, mV·h·ft^2/Btu (mV·m^2/W), and
T_{trans} = temperature of the transducer, °F (°C).

Each of the HFTs was calibrated for its sensitivity. The HFTs are very thin, have a large surface area and high conductivity, were placed between the drywall and the fiberglass insulation, and were attached to the drywall with heat sink gel. Consequently, the effect of HFT on the heat flux pattern through the ceiling is considered negligible. To ensure the accuracy of the HFTs, the heat flux values through the ceiling were also calculated from the thermocouple measurements and the estimated insulation R-values and compared to those obtained from the HFTs. The thermal conductivity of the fiberglass batt varies with temperature and thickness, so mean temperature and thickness were used to estimate the R-values as follows (Ober 1992):

$$R_{insu}^{-1} = \frac{K}{L} = \frac{4\,\sigma\,T_m^3}{\frac{1}{\varepsilon_1} + \frac{1}{\varepsilon_2} - 1 + \rho N L} + \frac{K_g}{L} \quad (4)$$

where

R_{insu} = thermal resistance of ceiling insulation, h·ft^2·°F/Btu (m^2·°C/W),
K = thermal conductivity of fiberglass batt, Btu·in./h·ft^2·°F (W/m^2·°C),
T_m = $(T_{s\text{-}bi} + + T_{s\text{-}ai})/2$ = mean temperature of fiberglass batt, °R (K),
L = thickness of fiberglass batt, in. (mm),
ϵ_1, ϵ_2 = emissivity of the surfaces of fiberglass batt = 0.9,
ρ = density of fiberglass batt, lb/ft^3 (kg/m^3),
N = scattering parameter, ft^3/lb·in. (m^3/kg·mm), and
K_g = air gas conductivity = $0.1804 \times [(T_m + 460°F)/535]^{0.906}$, Btu·in/h·ft^2·°F (0.1442 W·/m·°C).

The values of ρN were first calculated with Equation 4 using the nominal thicknesses of the fiberglass batts and the corresponding R-values. The ρN values were then used to obtain estimated R_{insu} at experimental thicknesses. The ceiling heat flux was then calculated by

$$Q_{ceil} = (T_{s\text{-}bi} - T_{s\text{-}ai}) / R_{insu} \quad (5)$$

where the variables have been previously defined for Equation 2.

The percentage reduction of heat flux due to the RB was calculated using the following equation:

$$\Delta Q / Q_0 = (Q_0 - Q) / Q_0 \quad (6)$$

where

Q_0 = heat flux when RB is not used, Btu/h·ft^2 (W/m^2),
Q = heat flux when RB is used, Btu/h·ft^2 (W/m^2).

In the experiment for determining the relative humidity levels beneath the radiant barrier, the wood samples utilized were oven-dried prior to placement at designated locations. Over a 20-day period, all samples were removed every five days, weighed, and then returned to their original locations. Sample weights were used to obtain moisture content on the oven-dried basis and, by reference to a published equilibrium moisture content table, the relative humidity was estimated.

RESULTS AND DISCUSSION

For heat flux determined by the HFTs, the maximum reduction (Table 2) due to the placement of an RB was 0.131 Btu/h·ft^2 (0.413 W/m^2), but this reduction was statistically insignificant at the 99% confidence level. This maximum occurred with an R-value of 19 h·ft^2·°F/Btu (3.32 m^2·°C/W), 0°F (-17.8°C), with the RB under the roof sheathing. The overall results showed no trend for the heat flux reductions with changes in R_{insu} and T_{out}.

There was no statistically significant difference in heat flux reduction at the 99% confidence level between the two RB locations (Figure 6).

The heat flux values at R-19 and R-38 calculated with Equation 3 from the HFTs were close to, but smaller than, those calculated with Equation 5 using thermocouple temperatures and estimated R-values (Figure 7). However, at R-57, the heat flux values from the HFTs were only about half as much as those from using temperature and estimated R-values.

The experiment to evaluate humidity levels under the RB showed no difference in the relative humidity on top of the insulation with and without RB (Figure 8). The relative humidity values were estimated from average temperatures and wood moisture contents, and a graphical record of the measured temperature over time is given in Figure 9. Frost was observed on the lower surface of the radiant barrier when T_{out} was 10°F (−12°C) or less.

The reduction in heat flux found experimentally due to the placement of an RB was very small, lower than those obtained from the theoretical calculations. One possible reason is the presence of ventilation in the experiments. As analyzed in the theoretical part, ventilation increases convective heat transfer and hence leads to a less effective RB. The quantity of ventilation in the experiment was hard to obtain due to the complexity of the airflow pattern in the freezer and attic space, but from Table 3 it can be seen that the values of T_a were very close to T_{out}, i.e., less than 1°F difference. The small difference between T_a and T_{out} indicates a high ventilation rate in the model house.

The heat flux reductions found in the experiment showed no trend with changes in R_{insu} and T_{out}. Possible factors contributing to this result are errors in HFT measurement and errors in insulation R-values. Since the effect of the errors on heat flux values could be relatively large compared to the small heat flux reductions due to the RB, the trend could have been masked.

The heat flux values measured by the HFTs were smaller than those based on calculations using thermocouple temperatures and estimated R-values. The differences between the two methods increased as R_{insu} increased and decreased as T_{out} decreased. At R-19 and R-38 levels of insulation, the differences of the heat flux measurements by the two methods were fairly small, while the difference was very large for R-57 ceiling insulation. The reason for this is believed to be the HFT measurement error. The sensitivity of the transducer is about 0.04 mV, while the reading from the HFT at R-57 was also about 0.04 mV.

The effectiveness of an RB system for reducing the heating load in a cold climate is less than that for the reduction of the cooling load in a warm climate. This can be attributed to the comparatively larger convective heat transfer coefficient when heat flow is upward, lower temperatures and smaller temperature differences between the two facing surfaces in the attic space, and the different contributions of attic ventilation. The perforations of the

TABLE 2
Heat Flux Values Showing the Effect of a Radiant Barrier as Measured by Heat Flux Transducer

R_{insu}	T_{out}	Q_{total}(Btu/hr·ft^2)			$\Delta Q(Q_0\text{-}Q)$		$\Delta Q/Q(\%)$	
	(°F)	No RB	$RB_{ceiling}$	RB_{roof}	$RB_{ceiling}$	RB_{roof}	$RB_{ceiling}$	RB_{roof}
	32	1.766	1.777	1.712	(0.011)	0.054	(0.6)	3.1
19	0	2.958	2.836	2.827	0.122	0.131	4.1	4.4
	-20	3.357	3.316	3.369	0.041	(0.012)	1.2	(0.3)
	32	0.915	0.921	0.944	(0.006)	(0.029)	(0.7)	(3.1)
38	0	1.562	1.480	1.441	0.082	0.121	5.2	7.7
	-20	1.858	1.729	1.844	0.129	0.014	6.9	0.8
	32	0.444	0.447	0.447	(0.003)	(0.003)	(0.5)	(0.5)
57	0	0.619	0.580	0.592	0.039	0.027	6.3	4.4
	-20	0.645	0.675	0.699	(0.030)	(0.054)	4.6	(8.2)

*1 Btu/hr·ft^2 = 3.1537 W/m^2

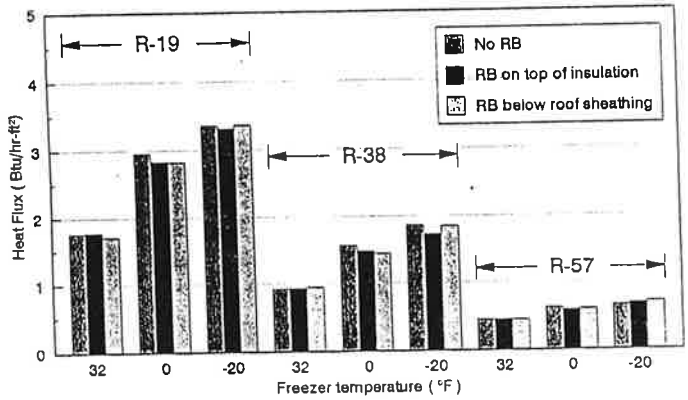

Figure 6 *Heat flux as measured by heat flux transducers.*

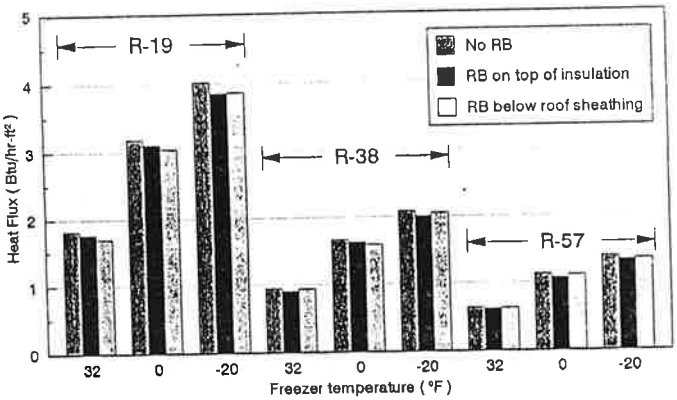

Figure 7 *Heat flux as calculated from measured temperatures and estimated insulation R-values.*

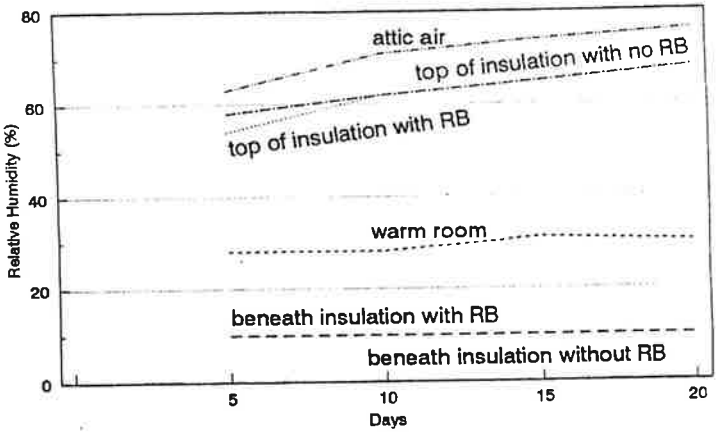

Figure 8 *Relative humidities at various locations as measured by wood samples.*

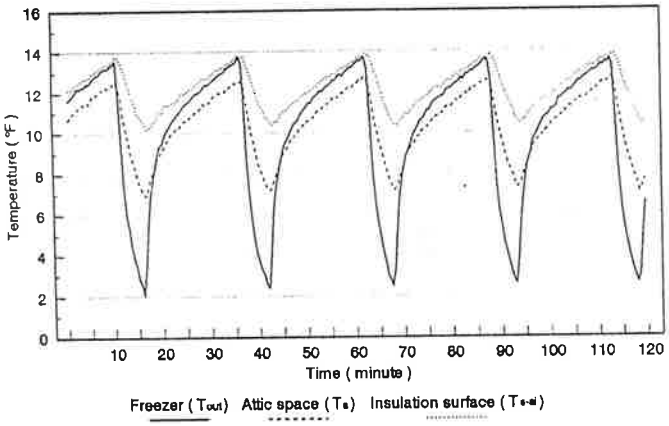

Figure 9 *Temperature fluctuations for an average freezer temperature of 10°F.*

radiant barrier used in this study did not allow adequate amounts of water vapor to escape from the thermal envelope as conditions got colder. Consequently, moisture/frost formed on the underside of the radiant barrier.

CONCLUSIONS

1. Both the theoretical and experimental results obtained from this research show that attic radiant barriers cause very low reductions in heating loads in a cold climate.
2. Theoretical calculations show that when the heat flux increases due to decreases in outside temperature and R-value of the ceiling insulation, the effectiveness of the radiant barrier increases. Experimentally, because of the small heat flux reductions due to the radiant barrier, this result was absent.
3. Experimentally, the heat flux reductions due to an attic radiant barrier as measured by the heat flux transducer were not statistically significant. However, the heat flux reductions as calculated from the use of thermocouple measurements, though very small, were statistically significant.
4. In a warm climate, ventilation has a positive effect on reducing the convective heat transfer from the attic air to the surface of the ceiling insulation by reducing attic temperature. Also, the coefficient of convective heat transfer is larger for heat flow upward than for heat flow downward. Both of these factors make an RB more effective for reducing cooling rather than heating loads.
5. Theoretically, the placement of the radiant barrier increased the temperature at the insulation top surface and hence increased convective heat transfer. This almost eliminated the reduction of radiative heat transfer.
6. Experimentally, when outside temperatures were below 10°F, water vapor condensed and frost developed on the bottom surface of the perforated radiant barrier.

ACKNOWLEDGMENTS

Funding for this project was by the Minnesota Legislature, grant no. MNADM/02140-03540, as recommended by the Legislative Commission on Minnesota Resources from the MENR Trust Fund. We extend our appreciation

TABLE 3
Temperatures (°F) at Various Locations as Measured by Thermocouples

		Tout	Ts-ar	Ts-br	Ta	Ts-ai	Ts-ad	Ts-bd	Tin
NO RB	R19	31.82	31.85	32.16	32.07	33.41	66.67	68.61	68.99
		0.11	0.32	0.94	0.94	4.09	65.60	68.20	68.96
		-19.32	-19.22	-18.41	-18.30	-15.45	64.96	67.77	68.52
	R38	32.07	32.14	32.62	32.33	32.88	67.33	68.50	68.78
		0.00	0.23	0.75	0.70	3.21	66.91	68.65	68.99
		-19.68	-19.36	-18.87	-19.04	-15.49	67.04	68.77	69.15
	R57	32.06	32.10	32.38	32.31	33.03	67.64	68.63	68.75
		-0.14	-0.14	0.36	0.22	3.00	67.68	69.02	69.11
		-19.70	-19.58	-18.93	-19.10	-14.52	67.48	68.67	68.55
$RB_{ceiling}$	R19	31.92	32.05	32.13	32.55	34.43	66.70	68.46	68.90
		0.18	0.28	0.68	1.16	6.28	65.88	68.34	69.11
		-19.11	-19.65	-19.11	-18.37	-11.05	65.44	68.18	68.87
	R38	32.42	32.29	32.59	32.65	35.17	67.65	68.51	68.78
		-0.58	-0.16	0.26	0.80	4.55	66.91	68.59	68.97
		-19.89	-19.57	-19.02	-18.66	-11.76	66.94	68.63	69.05
	R57	32.17	32.10	32.19	32.24	34.32	67.71	68.69	68.83
		-0.29	-0.21	0.34	0.62	7.07	67.69	68.80	69.01
		-19.57	-19.54	-19.08	-18.83	-9.86	67.89	69.03	68.93
RB_{roof}	R19	31.97	32.03	32.44	32.68	36.46	67.37	68.48	68.94
		0.68	0.96	1.39	2.06	7.96	66.29	68.14	68.95
		-19.63	-19.59	-19.18	-17.85	-11.46	65.27	68.13	68.83
	R38	32.16	32.12	32.23	32.39	33.26	67.33	68.52	68.79
		0.16	0.16	0.42	0.74	6.59	67.20	68.79	69.13
		-19.74	-19.50	-19.29	-18.57	-14.10	67.04	68.63	69.04
	R57	32.11	32.11	32.13	32.32	33.24	67.55	68.64	68.74
		0.12	0.37	0.58	1.09	4.32	67.66	68.78	68.93
		-19.88	-19.87	-19.58	-19.11	-11.41	67.87	69.05	68.90

* See Figure 5 for the locations of the thermocouples.

TABLE 4
Heat Flux Values Showing the Effect of a Radiant Barrier as Calculated from Measured Temperatures and Estimated R-Values

R_{insu}	T_{out}	Q_{total}(Btu/hr·ft^2)			$\Delta Q(Q_0-Q)$		$\Delta Q/Q$ (%)	
(hr·ft2·°F/Btu)	(°F)	No RB	$RB_{ceiling}$	RB_{roof}	$RB_{ceiling}$	RB_{roof}	$RB_{ceiling}$	RB_{roof}
	32	1.820	1.769	1.703	0.051	0.118	2.8	6.5
19	0	3.189	3.104	3.049	0.085	0.140	2.7	4.4
	-20	4.021	3.859	3.867	0.162	0.154	4.0	3.8
	32	0.949	0.899	0.939	0.050	0.01	5.3	1.1
38	0	1.664	1.632	1.593	0.031	0.070	1.9	4.2
	-20	2.085	2.001	2.054	0.084	0.030	4.0	1.5
	32	0.638	0.617	0.632	0.021	0.005	3.3	0.8
57	0	1.130	1.067	1.109	0.063	0.021	5.6	1.9
	-20	1.387	1.327	1.350	0.060	0.037	4.3	2.7

*1 Btu/hr·ft^2 = 3.1537 W/m^2

to David Ober, Bruce Nelson, Douglas Hawkins, and Thomas Kuehn for their contributions toward the research and this paper.

REFERENCES

DOE. 1991. Attic radiant barrier fact sheet. DOE/CE-0335P. Washington, DC: Department of Energy.

EKO. 1990. Operation manual for heat flow meters model CN-160A, B. Tokyo: EKO Instruments Trading Co., Ltd.

Forest, T.W. 1990. Evaluation of the performance of attic radiant barriers. Edmonton, Alberta, Canada: Department of Mechanical Engineering, University of Alberta.

Levins, W.P., and M.A. Karnitz. 1988. Heating energy measurements of single-family houses with attics containing radiant barriers in combination with R-11 and R-30 ceiling insulation. ORNL/CON-239. Oak Ridge, TN: Oak Ridge National Laboratory.

Lloyd, J.R., and W.R. Moran. 1974. Natural convection adjacent to horizontal surface of various platforms. ASME Paper No.74-WA/HT-66.

McQuiston, F.C., and J.D. Parker. 1988. *Heating, ventilating, and air conditioning*. New York: John Wiley & Sons, Inc.

Ober, D. 1992. Personal communication.